



Research Article

Preclinical Alternative Model for Analysis of Porous Scaffold Biocompatibility Applicable in Bone Tissue Engineering

Eva Petrovova¹, Maria Giretova², Alena Kvasilova³, Oldrich Benada⁴, Jan Danko¹, Lubomir Medvecky^{1,2} and David Sedmera^{3,5}

¹Institute of Anatomy, University of Veterinary Medicine and Pharmacy, Kosice, Slovak Republic; ²Institute of Materials Research, The Slovak Academy of Sciences, Kosice, Slovak Republic; ³Institute of Anatomy, Charles University, Prague, Czech Republic; ⁴Institute of Microbiology, The Czech Academy of Sciences, Prague, Czech Republic; ⁵Institute of Physiology, The Czech Academy of Sciences, Prague, Czech Republic

Abstract

Porous scaffolds represent a potential approach to repair critical-size bone defects. Vascularization is essential for bone formation and healing. This study establishes a method to monitor angiogenesis within porous biopolymer scaffolds made on the basis of polyhydroxybutyrate and chitosan. We used the chick and quail chorioallantoic membrane (CAM) assay as an alternative *in vivo* model to study the formation of new blood vessels inside the scaffold structure. The chemical properties of the biopolymer scaffold matrix surface were characterized as well as the tissue reaction of the CAM. Placing a piece of polymer scaffold on the CAM resulted in a vascular reaction documented visually and by ultrasound biomicroscopy. Histological analysis showed a myofibroblast reaction (smooth muscle actin-positive cells) without excessive collagen deposition. Cell invasion into the implant was observed and the presence of a vascular network was confirmed by identifying hemangioblasts and endothelial cells of quail origin using the QH1 marker. The CAM assay is a rapid and easy way to test biocompatibility and vasculogenic potential of new candidate scaffolds for bone tissue bioengineering while respecting the 3Rs.

1 Introduction

Regeneration maintains or renews the original tissue architecture. In case of damage or chronic degenerative disease, fibrotic repair occurs instead of the normal regenerative process. Such a response is considered a reparative process, since the replacement tissue neither contains the original cell types nor is the original tissue architecture reestablished (Stocum, 2002).

The term regenerative medicine is often used as a synonym for tissue engineering, though regenerative medicine focuses on using stem cells to form tissues, while tissue engineering makes use of a combination of cells, biochemical and physiochemical factors, and biomaterials to improve or replace biological functions (Langer and Vacanti, 1993). Many definitions of tissue engineering include a wide range of applications, however, in practice, tissue engineering closely focuses on repairing or replacing parts of or entire tissues (cartilage, bone, blood vessels, skin, muscle, nerves, etc.) including certain mechanical and structural properties that are required for proper functioning (Musumeci et al., 2014).

Angiogenesis is the physiological process of forming new capillaries from existing vessels. It is a tiered process involving activation of the existing endothelial cells, degradation of the extracellular matrix, proliferation and migration of endothelial cells, invasion of the stroma by the surrounding cells, and remodeling the extracellular matrix. Regulation of endothelial cell survival and migration strongly depends on the interaction of endothelial cells with extracellular matrix proteins via cell adhesion molecules, and the activities of growth factors and cytokines. Angiogenesis is characteristic of regeneration of normal tissues and hence is an important factor determining the safe and successful use of biomaterials in regenerative medicine (Chavakis and Dimmeler, 2002) as perfusion of the implant is needed to provide a feasible infrastructure upon which the new tissue can mature (Anderson et al., 2011). Induction of angiogenesis and subsequent development of a vascular bed in the engineered tissue is being actively pursued through combinations of physical and chemical cues, notably through the presentation of suitable topographies and growth factors (Klagsburn and Moses, 1999; Liu et al., 2012; Kant and Coulombe, 2018).

Received July 24, 2018; Accepted November 12, 2018; Epub November 23, 2018; © The Authors, 2018.

ALTEX 36(1), 121-130. doi:10.14573/altex.1807241

Correspondence: Eva Petrovova, DVM, PhD; Institute of Anatomy, University of Veterinary Medicine and Pharmacy, Komenského 73, 041 81 Kosice, Slovak Republic (eva.petrovova@uvlf.sk)

This is an Open Access article distributed under the terms of the Creative Commons Attribution 4.0 International license (<http://creativecommons.org/licenses/by/4.0/>), which permits unrestricted use, distribution and reproduction in any medium, provided the original work is appropriately cited.



Osteogenesis, the formation of bone, is closely connected with angiogenesis during the process of bone healing (Yu et al., 2017). One way to achieve a tissue-engineered bone tissue could be the use of an angiogenesis-promoting scaffold. Neovascularization into the implant not only supplies nutrients, oxygen, calcium, and phosphate, but also provides a transport route for the mesenchymal stem cells to facilitate bone regeneration (Stegen et al., 2015).

Scaffold that can promote osteogenesis and angiogenesis must have appropriate pore structure, biocompatibility, mechanical properties and processability to promote cell adhesion, migration, proliferation, and differentiation (Zhang et al., 2015). Chitosan is a hydrophilic biopolymer polysaccharide that induces and stimulates connective tissue rebuilding (Muzzarelli et al., 1988). It is a natural polymer with antibacterial properties that is biodegradable, biocompatible, highly abundant, and non-toxic. It can be molded into different forms (films, gels, sponges, fibers, nanoparticles, nanofibers) for diverse applications in tissue engineering (Concha et al., 2018; Poonguzhali et al., 2018). Because of the swelling of chitosan-based composites owing to water uptake during preparation, porous scaffold can be prepared by later lyophilization (Giretova et al., 2016). In bone tissue engineering, chitosan has frequently been used in combination with other bone-forming matrices such as hydroxyapatite or collagen (Tan et al., 2014). Poly-3-hydroxybutyrate (PHB) represents another natural, biodegradable and hydrophobic biopolymer that can be combined with chitosan or calcium phosphate to composites that are of interest for bone and cartilage regeneration and that may be suitable for the reconstruction of deeper defects.

The animal models play a key role in basic medical research. Advances in tissue engineering that lead to development of new therapeutic approaches are often based on *in vitro* experiments that are later followed by *in vivo* experiments. However, the use of rodents as model animals in experimental studies encounters ethical, practical and technical problems, which limit their use in certain areas of this research (Rashidi and Sottile, 2009). The avian embryo represents an easily available and cost-effective alternative model that may be used to test various biomaterials. Chicken or quail embryo development takes place outside the mother's body, obviating the need to sacrifice experimental animals or cause physical harm as is usually the case in implantation surgery. A further big advantage is that there is no need to apply for animal protocol approval for the chick/quail embryo *in ovo* as an experimental model as both are exempt from the horizontal legislation on the protection of animals used for scientific purposes in Europe (2010/63/EU), as well as applicable laws in the United States. The avian embryo, and especially its chorioallantoic membrane (CAM), thus provides a simple and effective alternative model to assess the biocompatibility of potential new bone implants (Kang et al., 2018; Tomco et al., 2017; Magnaudeix et al., 2016; Steffens et al., 2009) and can be considered a 3R method.

The CAM is used in many areas of research, including investigating molecules regulating the formation of blood vessels for use in the treatment of chronic inflammation, tumors, healing of wounds and fractures, drug delivery, and toxicological analysis (Hazel, 2003; Eun and Koh, 2004; Özçetin et al., 2013; Pandit et al., 2017; Ribatti, 2016). The CAM consists of two extra-embryonic membranes: the chorion and the allantois, which fuse

together on embryonic day (ED) 4. Histologically, the CAM is comprised of three layers: the ectoderm, mesoderm, and endoderm. It serves as a respiratory and excretory organ with a non-innervated, transparent matrix and a vascular network (Tay et al., 2012). On ED8, the proliferation and differentiation of blood vessels is already well advanced, forming an extensive and easily accessible arteriovenous system composed of the umbilical arteries and veins (Djonov et al., 2000), which can serve as a surrogate blood supply for organ culture, and hence a platform for biomaterial testing (Borges et al., 2003; Moreno-Jiménez et al., 2017). Over 700 publications have used the chick embryo CAM as a model system to study angiogenesis. More rarely, the Japanese quail CAM has also been used successfully (Buriková et al., 2016). A particular benefit of the quail CAM is that the quail-derived endothelium expresses the unique marker QH1, which can be identified using a specific antibody (Pardanaud et al., 1987; Drake et al., 1997; Brown et al., 1999; Giles et al., 2005; Sedmera and McQuinn, 2008).

In recent years, the field of tissue engineering has accepted the CAM model as a useful, quick, and cheap alternative to the traditional animal models (rabbit ears, rodent skin, avascular cornea of the rabbit, cheek pouches of the hamster; Ribatti et al., 2006; Da-Lozzo et al., 2013; Vargas et al., 2013) to evaluate angiogenesis in new implants and weed out less promising scaffold candidates, thus reducing or replacing *in vivo* animal experiments (Falkner et al., 2004).

This study describes a new approach to detect the formation of blood vessels inside biopolymer scaffolds using the CAM of the developing avian embryo as an alternative to traditional mammalian models, which would make this model particularly attractive for the rapid biocompatibility screening of porous biomaterials for regeneration of hard tissues.

2 Materials and methods

Preparation and characterization of composite scaffold

Polyhydroxybutyrate/chitosan scaffolds (PHB/CHIT) were prepared according to the method of Medvecky et al. (2014). Briefly, polyhydroxybutyrate (GoodFellow, Cambridge, England) dissolved in propylene carbonate (1% solution of PHB) and chitosan (Sigma Aldrich, middle, 1% solution in 1% acetic acid) were mixed together at a 1:1 ratio using a magnetic stirrer at 400 rpm. After 10 min of mixing, acetone (about 5 ml) was slowly added to the suspension to achieve precipitation of biopolymers. Final blends were filtered, washed with distilled water, and molded into a larger block (4×25×1 mm), which was then cut into smaller pieces with the final dimensions of 4×4×1 mm and lyophilized (Freeze dryer, iShin Biobase Europe, Ede, The Netherlands) for 6 h (Fig. 1). Swelling of the composite samples was measured in 1.5 ml vials by immersion of porous substrates (approximately 20 mg) in 0.9% NaCl solution at 37°C up to a constant mass. Soaking was done in triplicate and swelling was evaluated as the ratio of wet weight to dry weight. The microstructure of the scaffolds was observed by scanning electron microscopy (FE SEM JEOL7000). The phase analysis of the blend was evaluated by X-ray powder diffraction analysis (XRD, Philips X Pert Pro).

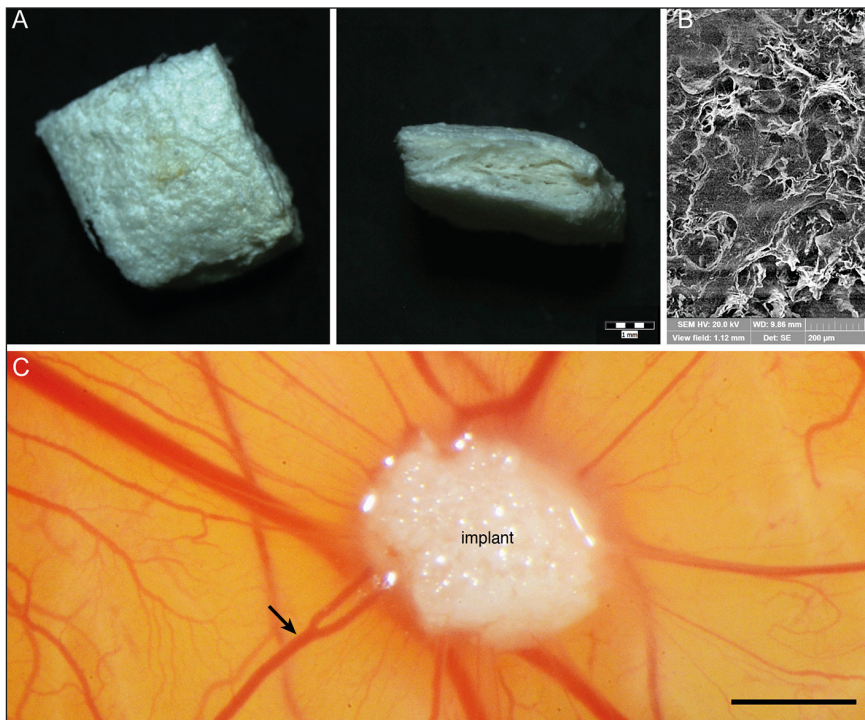


Fig. 1: Structure of PHB/CHIT scaffold and evidence of CAM blood vessels converging toward the implanted scaffold

(A) Macrostructure of PHB/CHIT scaffold, scale bar: 1 mm. (B) Ultrastructure of PHB/CHIT scaffold with pores (SEM), scale bar: 200 μm . (C) Macroscopic evidence of CAM blood vessels converging toward the implanted PHB/CHIT scaffold (arrows) on ED10; scale bar: 1 mm; 42 biological replicates (chick), 30 biological replicates (quail), for confirmatory images see¹.

¹ doi:10.14573/altex.1807241s1

Cytotoxicity testing

Cytotoxicity evaluation was carried out using MC3T3E1 mouse preosteoblasts (ECACC, Salisbury, UK) according to EN ISO 10993-5:2009. Cells were cultured in culture flasks in MEM (minimum essential medium) with Earl's balanced salts, 2 mM L-glutamine (SAFC Biosciences, Hampshire, UK), 10% fetal bovine serum (Sigma-Aldrich, St. Louis, MO, USA), and ATB-antimycotic (penicillin, streptomycin, amphotericin) solution (Sigma-Aldrich, St. Louis, MO, USA) at 37°C in 5% CO₂ at 95% humidity. After the cells reached about 80% confluence, they were harvested using 0.25% trypsin-EDTA (Sigma-Aldrich, St. Louis, MO, USA). Scaffold samples were sterilized in an autoclave at 121°C. Cell viability in the presence of scaffold samples was examined using the MTS test (Cell titer 96 aqueous one solution cell proliferation assay, Promega, Madison, WI, USA). The sterilized scaffolds (\varnothing 6 mm, thickness 1 mm, n = 5) were placed into the plate (treated 96-well tissue culture plate, cellGrade Brand, Wertheim, Germany), seeded with 1.0×10^4 MC3T3E1 mouse preosteoblasts in 200 μl complete osteogenic medium alpha modification MEM with 50 $\mu\text{g}/\text{ml}$ ascorbic acid, 50 nM dexamethasone, and 10 mM β -glycerophosphate (Sigma Aldrich, St. Louis, MO, USA) and cultured at 37°C in 5% CO₂ at 95% humidity. Cell viability in the presence of scaffolds was evaluated 2 and 10 days after cell seeding by measuring formazan concentrations produced by metabolically active cells in the culture medium using a UV-VIS spectrophotometer (Shimadzu, Griesheim, Germany) at a wavelength of 490 nm. The mean measured absorbance of medium from wells with cell-seeded substrates was compared with the absorbance of medium from scaffold-free wells (negative control, n = 5). The pure complete culture medium was used as a blank.

The attachment and morphology of cells were visualized by live/dead fluorescence staining using fluorescein diacetate/propidium iodide solution (green, live cells and red, dead cells) after 48 h of cell cultivation in the presence of scaffolds by an inverted optical fluorescence microscope (Leica DM IL LED, blue filter).

Chick CAM ex ovo model for microscopical evaluation

Avian embryos used in this study are exempt from Directive 2010/63/EU. Fertilized chicken hybrid eggs (Ross 308; n = 14) were purchased from the chicken farm of the Institute of Molecular Genetics (Koleč, Czech Republic) and delivered via courier in a temperature-controlled manner to ensure egg viability and quality. The eggs were incubated horizontally in a forced-draft constant-humidity incubator at 37.5°C and 60% relative humidity. At ED3 the eggshell was disinfected with 70% ethanol, then cracked and the egg content with chick embryo was carefully transferred into a hexagonal plastic weighing boat stored in a Petri dish partially filled with sterilized distilled water to maintain humidity, and incubated until ED6 in a still draft incubator (37.5°C, 70% relative humidity, without rocking; McQuinn et al., 2007).

On ED6, a piece (2 \times 2 \times 1 mm) of the sterilized porous scaffold (CHIT/PHB) was gently placed on the chorioallantoic membrane *ex ovo* using suture tying forceps.

For visual evaluation of vascular density and video blood flow observation into/outside the scaffold we used a stereomicroscope (Leica MZ125) fitted with a DSLR camera (D7000, Nikon, Tokyo, Japan) for video documentation on ED10. Blood contrast was enhanced using a green interference filter inserted into a KLD250 halogen light source. Ultrasound biomicroscopy examination of implants was performed *ex ovo* on a high-resolution imaging system Vevo 770 (VisualSonics, Toronto, Canada) using



B-Mode imaging (scanhead #708), which allows the acquisition of two-dimensional images of the vessels inside of scaffolds as well as blood flow monitoring in a temperature-controlled setup (McQuinn et al., 2007).

Quail CAM in ovo model for evaluation of angiogenesis and biocompatibility

For implantation of scaffolds on the quail CAM *in ovo*, we used a method modified from Ribatti et al. (2006). Fertilized Japanese quail (*Coturnix japonica*) eggs ($n = 10$) were purchased from the animal farm (Kosice, Slovakia) and delivered via courier in a temperature-controlled manner to ensure egg viability and quality. The eggs were incubated with blunt end up in a forced-draft constant-humidity incubator at 37.5°C and 60% relative humidity with continuous rocking. At ED3 the eggs were windowed on the blunt end, and the inner shell membrane (*membrana papyracea*) was carefully removed. The windows were closed using insulation tape and returned to a still draft incubator.

On ED5, a sterilized porous scaffold (CHIT/PHB) was gently placed on the chorioallantoic membrane, and the opening was re-sealed with the insulation tape. On ED10, Dent's solution was applied directly onto the CAM with the scaffold and surrounding vessels for 10 min at room temperature. Subsequently, the implant was removed and processed for evidence of angiogenesis and biocompatibility with histological techniques.

Scanning electron microscopy (SEM)

SEM analysis was used to investigate whether CAM microvilli grow into the pores of the scaffold. This would evidence biocompatibility of the tested biomaterial. *In ovo* implants at ED10 were fixed with 1% glutaraldehyde and 2% formaldehyde in PBS for 24 h at 4°C, rinsed three times with PBS, and then post-fixed in 1% osmium tetroxide. After further rinsing, the specimens were dehydrated with ethanol series, critical point dried with CO₂, and mounted on aluminum stubs. After sputter coating with gold, they were observed under a Bruker scanning electron microscope.

Histological examination

The monitoring of the implant reaction and biocompatibility with the surrounding CAM was carried out using routine H&E/Alcian Blue staining, followed by scanning of the slides using a 10x objective on an Olympus slide scanner.

The presence of myofibroblasts and macrophages (α -SMA, collagen I and CD68, respectively) as well as proliferative activity of the cells within the implant (phosphohistone-3, Anti-H3S10p) was evaluated with immunohistochemical staining of chick embryos. Deparaffinized sections were blocked in normal goat serum (1:10) and in 1% bovine serum albumin (BSA) in PBS with 0.1% Triton-X (Sigma-Aldrich, St. Louis, USA) for 60 min at RT. For staining with CD68 antibody, collagen I, and anti-H3S10p, antigen retrieval was performed with 10 mM citrate buffer (pH 6) in a microwave oven (750 W) for two cycles of 5 min each prior to immunostaining. Primary antibodies (monoclonal mouse antibody α -SMA, 1:800, Sigma-Aldrich # A2547; polyclonal rabbit anti-mouse antibody collagen type I, 1:500, MDBiosciences, Oakdale, USA; monoclonal mouse antibody CD68, 1:100, Abcam ab955, Cambridge, UK or polyclonal rabbit antibody anti-H3S10p,

1:100, Millipore, CA, USA) were applied overnight at +4°C. Negative controls were obtained by omission of the primary antibody. The sections were then washed in PBS, and TRITC-conjugated goat anti-mouse secondary antibody or goat anti-rabbit secondary antibody for collagen type I (1:200, Jackson ImmunoResearch Laboratory, West Grove, PA, USA) was applied for 90 min in the dark at RT. Together with the secondary antibody, wheat germ agglutinin (WGA) coupled with the Alexa 488 dye was applied at 1:100 concentration to detect fibrous extracellular matrix including collagen (Benes et al., 2011). After washing in PBS, the nuclei were counterstained with Hoechst 33258 (1:100,000 diluted in 0.1% Triton-X in distilled water, Sigma-Aldrich, St. Louis, MO, USA). The sections were washed with distilled water and dehydrated in ethanol series, cleared in xylene, and mounted in DEPEX (Electron Microscopy Sciences, Hatfield, PA, USA).

The presence of hemangioblasts and endothelial cells was investigated with QH1 staining. Deparaffinized sections of ten quail embryos with implants were blocked in normal goat serum (1:10) and in 1% bovine serum albumin (BSA) in PBS with 0.1% Triton-X (Sigma-Aldrich, St. Louis, MO, USA) for 60 min at RT. QH1 (monoclonal mouse antibody, 1:1000, DSHB, Iowa, USA) was then applied overnight at +4°C. Negative controls were obtained by omission of the primary antibody. The sections were washed in PBS and TRITC-conjugated goat anti-mouse secondary antibody (Jackson ImmunoResearch Laboratory, West Grove, PA, USA) was applied for 4 h in the dark at RT. After washing in PBS, the nuclei were counterstained with Hoechst 33258 (1:100,000 diluted in 0.1% Triton-X in distilled water, Sigma-Aldrich, St. Louis, MO, USA). The sections were washed with distilled water and dehydrated in ethanol series, cleared in xylene, and mounted in permanent medium.

Fluorescently stained sections were examined first on a wide-field epifluorescence microscope (Olympus BX51) and then documented on a confocal microscope Olympus FV-1000 BX61 (Olympus, Tokyo, Japan). Images were assembled and labeled using Adobe Photoshop (version 8.0) using Wiley standards for digital image manipulation. Brightness and contrast were adjusted using the "Adjust Levels" command on the entire image, and "Unsharp Mask" filter was used where necessary to enhance sharpness. No other image manipulations were performed.

CAM tissue remodeling in relation to the implanted scaffold was further analyzed using picrosirius red staining according to Junqueira et al. (1979). This specific staining of extracellular collagen fiber deposition was combined with immunohistochemical staining of WGA coupled with the Alexa 488 dye (1:100), and the nuclei were counterstained with Hoechst 33258 (1:100,000 diluted in 0.1% Triton-X in distilled water). For histological and immunofluorescent studies, we used 4 sections per slide, 2 slides per sample.

3 Results

3.1 Properties, microstructure and *in vitro* cytotoxicity of composite scaffolds

A macroporous microstructure with high fractions of spherical pores, which did not exceed 80 μ m diameter, and irregular macropores, with diameters up to 150 μ m, was observed in PHB/CHIT

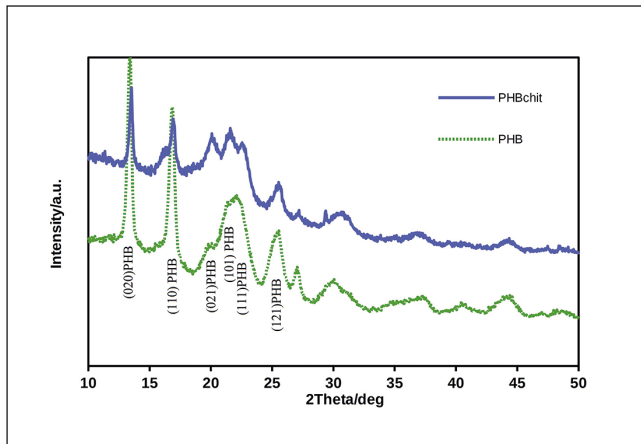


Fig. 2: XRD patterns of PHB and PHB/CHIT blend
Biological replicates (4).

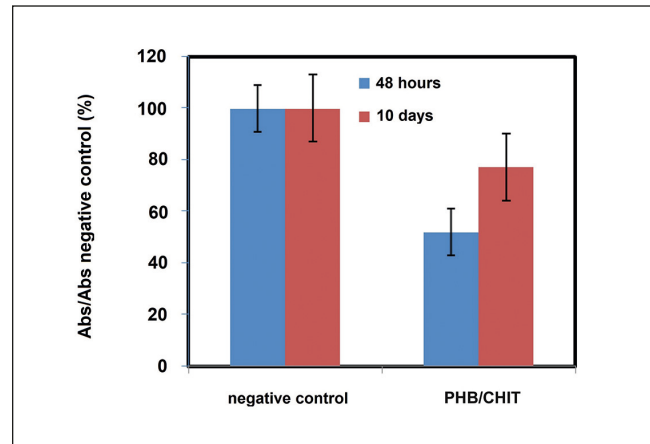


Fig. 3: Proliferation of osteoblasts on PHB/CHIT scaffolds in relation to negative control after 2 and 10 days of cell cultivation

Biological replicates (6), $p < 0.01$ (one-way ANOVA, $\alpha = 0.05$, StatMost statistical software).

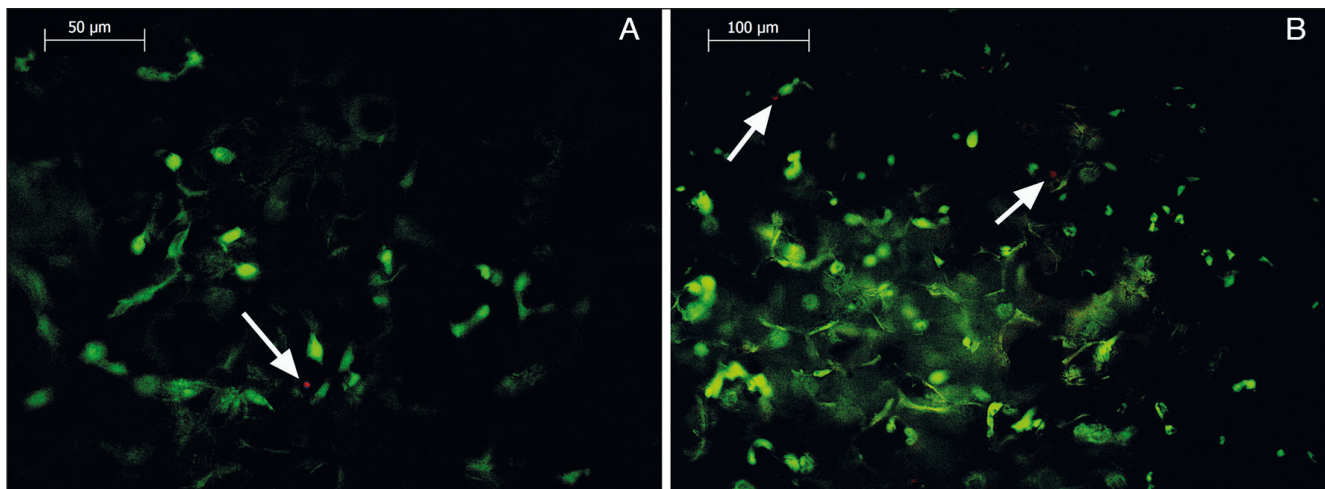


Fig. 4: Live/dead (arrows) fluorescence staining of cells growing on scaffolds after 2 days of cultivation

Biological replicates (9), technical replicates (45), for confirmatory images see³. Because of the porous structure of the material and non-standard conditions for observation of cells by optical microscopy (especially flat surface), full images were not sharpened.

scaffolds (Fig. 1) by SEM. These pore sizes appear appropriate for migration of cells into the inner structure of the scaffolds to form specific tissues. No clearly distinguishable biopolymer fibers were visible in the detailed micrograph, which demonstrates uniform and homogeneous distribution of both biopolymers in the blend.

Dimensions of individual fibers have to be sufficient for crystallization into coherent regions, which was demonstrated by the XRD analysis (Fig. 2). The strong lines from reflections of (020), (110), (101), and (121) PHB planes verify a higher fraction of the crystalline PHB component in the PHB/CHIT blend contrary to the amorphous character of chitosan. A significant reduction of the average molecular mass of chitosan from 360 kDa to about 41 kDa was found after precipitation of biopolymers, which is probably the reason for low chitosan crystallinity.

A fast increase in scaffold mass was observed after the first 2 h of soaking when the mass increment achieved about 90% of the final water uptake. Constant mass of samples was reached after 2 days of swelling at which the dry mass of the biopolymer scaffold had more than doubled. This confirmed a highly hydrophilic character of the blend, which supports the adsorption of polar molecules (like nutrients, etc.) from the surrounding medium including body fluids.

Formazan production of preosteoblasts in contact with the scaffolds for 2 and 10 days of culture (results not shown) indicated an increase in the number of viable cells (about 7-fold), which demonstrates that the scaffolds support cell growth. The relative viability of cells increased from 50% after 2 days of culture to around 80% of the negative control after 10 days of culture, which confirms a non-cytotoxic behavior of biopolymer scaffolds (EN

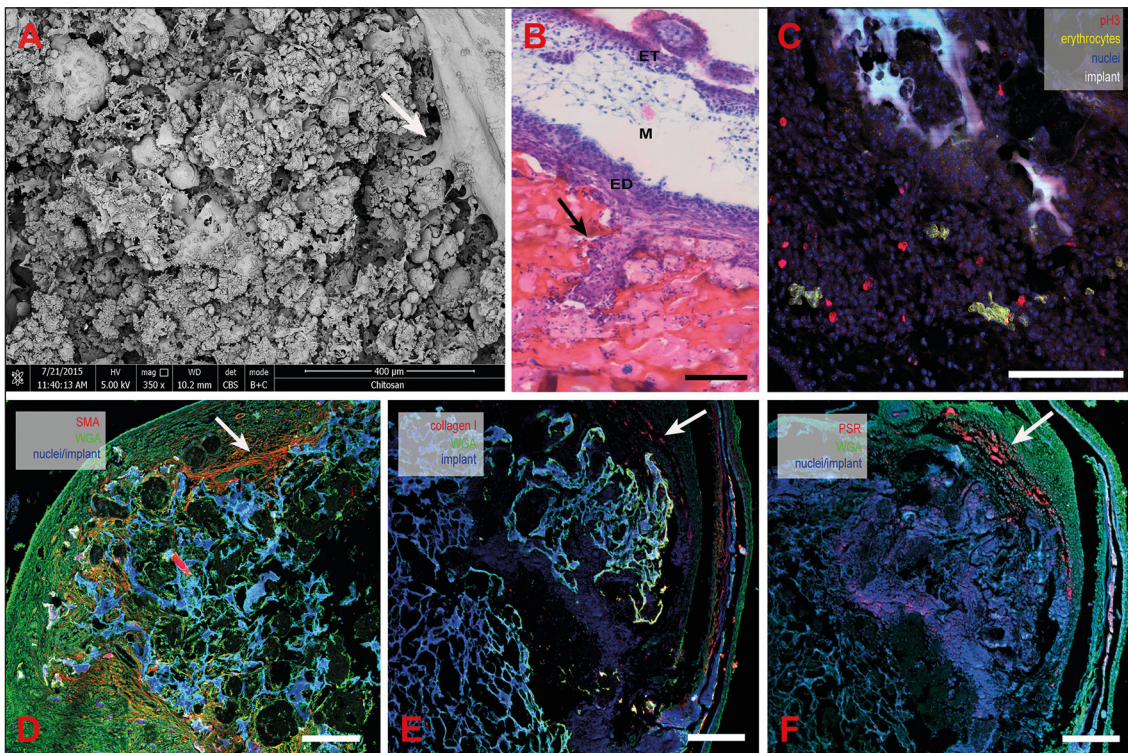


Fig. 5: Immunohistochemical analysis of the implant after 5 days *in ovo*

(A) Histology of the implant after 5 days *in ovo*. The formation of CAM villi growing into the implanted PHB/CHIT scaffold was observed using SEM as a comparison with histology (3D); scale bar: 400 μ m. (B) Confirmation of CAM villi presence with H-E/Alcian blue staining; ET, ectoderm; M, mesoderm; ED, endoderm; scale bar: 100 μ m. (C) Evidence of CAM tissue and proliferating cells within implanted scaffold; scale bar: 100 μ m. (D) The presence of myofibroblasts on a border between scaffold and surrounding CAM tissue; scale bar: 100 μ m. (E, F) Collagen was localized around implant without its excessive deposition; scale bar: 200 μ m; biological replicates (15), technical replicates (720), for confirmatory images see¹.

ISO 10993-5; Fig. 3). Images from live/dead fluorescence staining (Fig. 4) documented good adherence of cells to pore walls of scaffolds 2 days after seeding. The live cells' visible filopodia copied the pore walls and only few dead cells were observed (stained red; panel A, B of Fig. 4).

3.2 Incorporation of scaffold into the CAM

Five days after placing the PHB/CHIT scaffold on the CAM, it was well incorporated. Hyperplasia of the CAM tissue under the scaffold was observed in all cases. Epithelial cells from the CAM ectoderm were observed to proliferate and move into the PHB/CHIT component, forming fusion boundaries between the scaffold and CAM tissues, suggesting good biocompatibility and bioactivity of this biomaterial. Newly formed CAM tissue was observed also within the PHB/CHIT scaffold as the formation of CAM villi. These cells expressed smooth muscle actin, suggesting they were myofibroblasts. They were localized only in some areas around the implant. However, there was no excessive production of collagen I or extracellular matrix as revealed by WGA or pi-

crossorius red staining (Fig. 5). CD68 staining did not identify the presence of macrophages.

3.3 Angiogenesis within the scaffolds on the CAM

Endothelial cell migration and sprouting are the most important steps of angiogenesis. We observed vessels leading to and from the implant on the surface of the CAM (Fig. 1), suggesting its vascularization after 5 days of implantation. This was confirmed by high-resolution videomicroscopy (Video S2²) and ultrasound biomicroscopy (Video S3³). The presence of endothelial precursors and vessels inside the implant was confirmed by positive QH1 staining (Fig. 6) on scaffolds implanted into the quail chorioallantoic membrane.

4 Discussion

Cell adhesion to an implant and cell activity are influenced by properties of the implant surface such as surface tension, roughness,

² *In situ* blood flow from the PHB/CHIT implanted scaffold including the vessels: doi:10.14573/altex.1807241s2

³ Blood flow inside of PHB/CHIT implanted scaffold by VeVo ultrasound system: doi:10.14573/altex.1807241s3

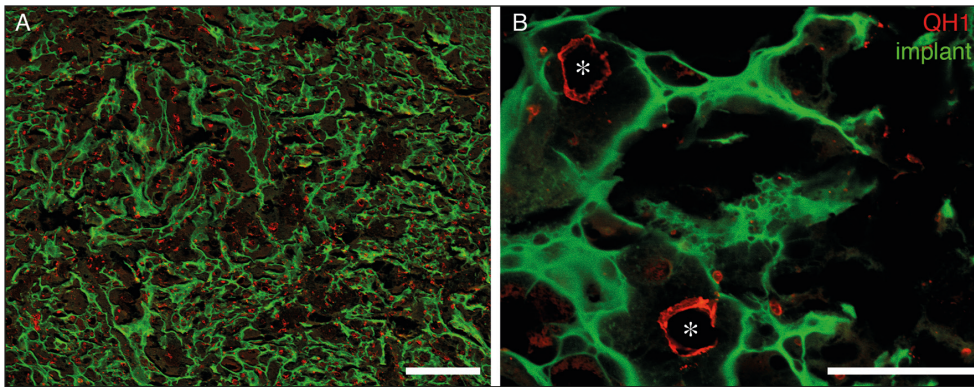


Fig. 6: Evidence of endothelial cells, hemangioblasts, and blood vessels inside the implanted scaffold

(A) QH1 positive endothelial cells; scale bar: 200 μm . (B) Blood vessels (asterisk) and hemangioblasts are present inside of implanted scaffold; scale bar: 100 μm ; biological replicates (9), technical replicates (72), for confirmatory images see¹.

etc. (Wang et al., 2005). Chitosan provides a reservoir for the release of bioactive substances and also acts as a scaffold that is amenable to colonization by cells (Barreto et al., 2016; Medvecký et al., 2014).

Polyhydroxybutyrate porous scaffolds in combination with biphasic calcium phosphate or chitosan are known to stimulate proliferation of fibroblasts and osteoblasts without inducing a proinflammatory response (Cool et al., 2007; Veleirinho et al., 2012; Tai et al., 2014). The average molecular weight of chitosan decreases after precipitation in propylene carbonate solution, but this does not appear to have negative effects as Giretova et al. (2016) found that lysozyme-degraded scaffolds containing a large fraction of low molecular weight chitosan (LMWC) were not cytotoxic even after 10 days of cultivation.

Previous studies have reported that various versions of chitosan-based scaffolds may support angiogenesis for different applications (Deng et al., 2010; Wang et al., 2012; Linn et al., 2003; Agarwal et al., 2016; Shahzadi et al., 2016); however only few studies have investigated this for the field of bone tissue engineering and these were only able to show evidence of angiogenesis on the scaffold surface (Pan et al., 2018; Ahmadi et al., 2010) or found that chitosan-acetate may actually inhibit angiogenesis (Shah et al., 2014). Others have attempted to enhance angiogenesis by loading chitosan scaffolds with recombinant vascular endothelial growth factor (VEGF) (Linn et al., 2003) or expressing VEGF with an adenoviral vector (Koç et al., 2014).

We here show clear evidence of blood vessel ingrowth into unseeded PHB/CHIT scaffolds without performing *in vivo* testing on animals and without expression or addition of VEGF. Using the QH1 antibody, we observed the presence of individual endothelial cells as well as vessels inside the porous biomaterial. However, there are also some QH1-positive cells not connected to the vessels. It is thus possible that hemangioblasts migrate into the implant and vasculogenesis takes place together with angiogenesis. This hypothesis would have to be tested by another experimental study.

We found that the chitosan implant surface has fibrotic effects, probably because the implant surface directly activates quiescent myofibroblasts to differentiate into myofibroblasts by providing a mechanical stimulus. Myofibroblasts are characterized by an excessive production of collagen (Majd et al., 2015). Using WGA labeling of extracellular matrix, which was found to be comparable with the established picrosirius red staining, we found

that the fibrous layer was present around the implant outside of the layer of α -smooth muscle actin (α -SMA) positive myofibroblasts (Fig. 4; Emde et al., 2014).

We did not find evidence of induction of a non-specific inflammatory reaction by the implant as we did not find an influx of CD68 positive macrophages. This may be because we put the implant on the CAM early during development (ED5), at a time when the immune system is still immature. Inflammatory angiogenesis, in which infiltrating macrophages are the source of angiogenic factors, has to be distinguished from direct angiogenic activity of the tested biomaterial with histological analysis and immunohistochemical staining for specific cell populations. It would be interesting to extend our studies also into the later period (Bauguera et al., 2012) to monitor myofibroblasts as they become apoptotic or fibrosis develops, and to observe the influx of macrophages as the immune system develops. However, in some countries protection of the avian embryo starts at ED12-14 when the nervous system develops sensory synapses and two thirds of gestation has elapsed.

The CAM was previously used as an *in ovo* method for evaluating the tissue response to various biomaterials, including composites based on collagen (Vargas et al., 2013), Elvax 40 (ethylene-vinyl acetate copolymer; Langer and Folkman, 1976), hydron (poly-2-hydroxyethyl-methacrylate polymer; HydroMed; Ribatti et al., 1996), PCL (polycaprolactone; Singh et al., 2012), and matrix hydrogels (Fercana et al., 2017). This is a rather low-tech method, which makes it possible to continuously monitor angiogenesis, to easily and quickly obtain results, and to evaluate them in a relatively short time period. The response of the CAM to a biomaterial is similar to that of the mammalian animal model. However, in contrast to the mammalian model, it allows continuous monitoring, which makes it very attractive for rapid *in ovo/ex ovo* angiogenesis evaluation (Magnaudeix et al., 2016; Jin et al., 2016). Angiogenesis in the CAM model is usually quantified by assessing the number of new vessels oriented towards the implant (Ribatti et al., 2006; Strick et al., 1991). This method is rather subjective and only considers angiogenesis outside or on the surface of the scaffold. The focus of our study was primarily to identify the presence of blood vessels in the internal structure of the scaffold.

Our results showed that the PHB/CHIT scaffold has satisfactory angiogenic properties and induces formation of CAM villi



penetrating the pores of the implant. One can easily quantify the number of blood vessels in the vicinity of the implant, perform topographical and structural assessment using confocal or electron microscopy, and examine the cellular changes within the structure by immunohistochemistry.

The CAM model represents an intermediate step for testing biomaterial between the simple, *in vitro* model and the complex *in vivo* mammalian animal model (Valdes et al., 2002). Thus, it can reduce and replace animal experiments in the field of bone regenerative medicine.

5 Conclusions

Original porous PHB/CHIT biomaterial designed for bone regeneration was tested for the first time with a short-term CAM assay. Previous studies monitored the pro-angiogenic properties and biocompatibility only on the surface of similar porous scaffolds based on chitosan. In this study, the methods were focused on monitoring of angiogenesis and biocompatibility inside of the scaffold, which provides more complex information for the qualitative assessment of the tested biomaterial. The methods allow observation of the surrounding CAM tissue reaction, presence of cells in the pores of the scaffold, and the comparison of vessels growing toward the implant with their actual presence inside it. The presence of hemangioblasts and endothelial cells inside the scaffold could be shown. It remains to be determined whether angiogenesis or vasculogenesis is involved. Myofibroblasts were found around the implant, but without excessive collagen deposition. This study confirmed that the CAM assay is a rapid, cost-effective and simple method to test and optimize new scaffolds before their use on larger experimental animals.

References

- Agarwal, T., Narayan, R., Maji, S. et al. (2016). Gelatin/carboxymethyl chitosan based scaffolds for dermal tissue engineering applications. *Int J Biol Macromol* 93, 1499-1506. doi:10.1016/j.ijbiomac.2016.04.028
- Ahmadi, R., Burns, A. J. and de Bruijn, J. D. (2010). Chitosan-based hydrogels do not induce angiogenesis. *J Tissue Eng Regen Med* 4, 309-315. doi:10.1002/term.247
- Anderson, S. M., Siegman, S. N. and Segura, T. (2011). The effect of vascular endothelial growth factor (VEGF) presentation within fibrin matrices on endothelial cell branching. *Biomaterials* 32, 7432-7443. doi:10.1016/j.biomaterials.2011.06.027
- Baiguera, S., Macchiarini, P. and Ribatti, D. (2012). Chorioallantoic membrane for *in vivo* investigation of tissue-engineered construct biocompatibility. *J Biomed Mater Res Part B* 100, 1425-1434. doi:10.1002/jbm.b.32653
- Barreto, R. S., Quintans, J. S., Barreto, A. S. et al. (2016). Improvement of wound tissue repair by chitosan films containing (-)-borneol, a bicyclic monoterpene alcohol, in rats. *Int Wound J* 13, 799-808. doi:10.1111/iwj.12385
- Benes Jr., J., Melenovsky, V., Skaroupkova, P. et al. (2011). Myocardial morphological characteristics and proarrhythmic substrate in the rat model of heart failure due to chronic volume overload. *Anat Rec* 294, 102-111. doi:10.1002/ar.21280
- Borges, J., Tegtmeier, F. T., Padron, N. T. et al. (2003). Chorioallantoic membrane angiogenesis model for tissue engineering: A new twist on a classic model. *Tissue Eng* 9, 441-450. doi:10.1089/107632703322066624
- Brown, C. B., Drake, C. J. and Barnett, J. V. (1999). Antibodies directed against the chicken type II TGFbeta receptor identify endothelial cells in the developing chicken and quail. *Dev Dyn* 215, 79-85. doi:10.1002/(SICI)1097-0177(199905)215:1<79::AID-DVDY9>3.0.CO;2-H
- Buriková, M., Bilčík, B., Máčajová, M. et al. (2016). Hypericin fluorescence kinetics in the presence of low density lipoproteins: Study on quail CAM assay for topical delivery. *Gen Physiol Biophys* 35, 459-468. doi:10.4149/gpb_2016014
- Chavakis, E. and Dimmeler, S. (2002). Regulation of endothelial cell survival and apoptosis during angiogenesis. *Arterioscler Thromb Vasc Biol* 22, 887-893. doi:10.1161/01.ATV.0000017728.55907.A9
- Concha, M., Vidal, A., Giacaman, A. et al. (2018). Aerogels made of chitosan and chondroitin sulfate at high degree of neutralization: Biological properties toward wound healing. *J Biomed Mater Res B Appl Biomater* 106, 2464-2471. doi:10.1002/jbm.b.34038
- Cool, S. M., Kenny, B., Wu, A. et al. (2007). Poly(3 hydroxybutyrate-co-3-hydroxyvalerate) composite biomaterials for bone tissue regeneration: *In vitro* performance assessed by osteoblast proliferation, osteoclast adhesion and resorption, and macrophage proinflammatory response. *J Biomed Mater Res* 82, 599-610. doi:10.1002/jbm.a.31174
- Da-Lozzo, E. J., Moledo, R. C., Faraco, C. D. et al. (2013). Curcumin/xanthan-galactomannan hydrogels: Rheological analysis and biocompatibility. *Carbohydr Polym* 93, 279-284. doi:10.1016/j.carbpol.2012.02.036
- Deng, C., Zhang, P., Vulesevic, B. et al. (2010). A collagen-chitosan hydrogel for endothelial differentiation and angiogenesis. *Tissue Eng Part A* 16, 3099-3109. doi:10.1089/ten.tea.2009.0504
- Djonov, V., Schmid, M., Tschanz, S. A. and Burri, P. H. (2000). Intussusceptive angiogenesis: Its role in embryonic vascular network formation. *Circ Res* 86, 286-292. doi:10.1161/01.RES.86.3.286
- Drake, C. J., Brandt, S. J., Trusk, T. C. and Little, C. D. (1997). TAL1/SCL is expressed in endothelial progenitor cells/angioblasts and defines a dorsal-to-ventral gradient of vasculogenesis. *Dev Biol* 192, 17-30. doi:10.1006/dbio.1997.8751
- Emde, B., Heinen, A., Gödecke, A. and Bottermann, K. (2014). Wheat germ agglutinin staining as a suitable method for detection and quantification of fibrosis in cardiac tissue after myocardial infarction. *Eur J Histochem* 58, 2448. doi:10.4081/ejh.2014.2448
- Eun, J. P. and Koh, G. Y. (2004). Suppression of angiogenesis by the plant alkaloid, sanguinarine. *Biochem Biophys Res Commun* 317, 618-624. doi:10.1016/j.bbrc.2004.03.077
- Falkner, E., Eder, C., Kapeller, B. et al. (2004). The mandatory CAM testing of cells and scaffolds for tissue engineering: Benefits for the three Rs of cooperation with the vaccine industry. *Altern Lab Anim* 32, 573-580.
- Fercana, G. R., Yemeni, S., Billaud, M. et al. (2017). Perivascular extracellular matrix hydrogels mimic native matrix microarchi-

- ture and promote angiogenesis via basic fibroblast growth factor. *Biomaterials* 123, 142-154. doi:10.1016/j.biomaterials.2017.01.037
- Giles, P. B., Candy, C. L., Fleming, P. A. et al. (2005). VEGF directs newly gastrulated mesoderm to the endothelial lineage. *Dev Biol* 279, 169-178. doi:10.1016/j.ydbio.2004.12.011
- Giretova, M., Medvecky, L., Stulajterova, R. et al. (2016). Effect of enzymatic degradation of chitosan in polyhydroxybutyrate/chitosan/calcium phosphate composites on in vitro osteoblast response. *J Mater Sci Mater Med* 27, 181. doi:10.1007/s10856-016-5801-7
- Hazel, S. J. (2003). A novel early chorioallantoic membrane assay demonstrates quantitative and qualitative changes caused by antiangiogenic substances. *J Lab Clin Med* 141, 217-228. doi:10.1067/mlc.2003.19
- Jin, K., Ye, X., Li, S. et al. (2016). A biomimetic collagen/heparin multi-layered porous hydroxyapatite orbital implant for in vivo vascularization studies on the chicken chorioallantoic membrane. *Graefes Arch Clin Exp Ophthalmol* 254, 83-89. doi:10.1007/s00417-015-3144-6
- Junqueira, L. C., Bignolas, G. and Brentani, R. R. (1979). Picrosirius staining plus polarization microscopy, a specific method for collagen detection in tissue sections. *Histochem J* 11, 447-455. doi:10.1007/BF01002772
- Kang, M. S., Lee, N. H., Singh, R. K. et al. (2018). Nanocements produced from mesoporous bioactive glass nanoparticles. *Biomaterials* 162, 183-199. doi:10.1016/j.biomaterials.2018.02.005
- Kant, R. J. and Coulombe, K. L. K. (2018). Integrated approaches to spatiotemporally directing angiogenesis in host and engineered tissues. *Acta Biomater* 69, 42-62. doi:10.1016/j.actbio.2018.01.017
- Klagsburn, M. and Moses, M. A. (1999). Molecular angiogenesis. *Chem Biol* 6, 217-224. doi:10.1016/S1074-5521(99)80081-7
- Koç, A., Finkenzeller, G., Elçin, A. E. et al. (2014). Evaluation of adenoviral vascular endothelial growth factor-activated chitosan/hydroxyapatite scaffold for engineering vascularized bone tissue using human osteoblasts: In vitro and in vivo studies. *J Biomater Appl* 29, 748-760. doi:10.1177/0885328214544769
- Langer, R. and Folkman, J. (1976). Polymers for the sustained release of proteins and other macromolecules. *Nature* 263, 797-800. doi:10.1038/263797a0
- Langer, R. and Vacanti, J. P. (1993). Tissue engineering. *Science* 260, 920-926. doi:10.1126/science.8493529
- Linn, T., Erb, D., Schneider, D. et al. (2003). Polymers for induction of revascularization in the rat fascial flap: Application of vascular endothelial growth factor and pancreatic islet cells. *Cell Transplant* 12, 769-778. doi:10.3727/000000003108747244
- Liu, X., Wang, X., Horii, A. et al. (2012). In vivo studies on angiogenic activity of two designer self-assembling peptide scaffold hydrogels in the chicken embryo chorioallantoic membrane. *Nanoscale* 4, 2720-2727. doi:10.1039/c2nr00001f
- Magnaudeix, A., Usseglio, J., Lasgorceix, M. et al. (2016). Quantitative analysis of vascular colonisation and angiogenesis in porous silicon-substituted hydroxyapatite with various pore shapes in a chick chorioallantoic membrane (CAM) model. *Acta Biomater* 38, 179-189. doi:10.1016/j.actbio.2016.04.039
- Majd, H., Scherer, S. S., Boo, S. et al. (2015). Novel micropatterns mechanically control fibrotic reactions at the surface of silicone implants. *Biomaterials* 54, 136-147. doi:10.1016/j.biomaterials.2015.03.027
- McQuinn, T. C., Bratoeva, M., deAlmeida, A. et al. (2007). High-frequency ultrasonographic imaging of avian cardiovascular development. *Dev Dyn* 236, 3503-3513. doi:10.1002/dvdy.21357
- Medvecky, L., Giretova, M. and Stulajterova, R. (2014). Properties and in vitro characterization of polyhydroxybutyrate-chitosan scaffolds prepared by modified precipitation method. *J Mater Sci Mater Med* 25, 777-789. doi:10.1007/s10856-013-5105-0
- Moreno-Jiménez, I., Kanczler, J. M., Hulsart-Billstrom, G. et al. (2017). The chorioallantoic membrane assay for biomaterial testing in tissue engineering: A short-term in vivo preclinical model. *Tissue Eng Part C Methods* 23, 938-952. doi:10.1089/ten.tec.2017.0186
- Musumeci, G., Castrogiovanni, P., Leonardi, R. et al. (2014). New perspectives for articular cartilage repair treatment through tissue engineering: A contemporary review. *World J Orthop* 5, 80-88. doi:10.5312/wjo.v5.i2.80
- Muzzarelli, R., Baldassarre, V., Conti, F. et al. (1988). Biological activity of chitosan. Ultrastructural study. *Biomaterials* 9, 247-252. doi:10.1016/0142-9612(88)90092-0
- Özçetin, A., Aigner, A. and Bakowsky, U. (2013). A chorioallantoic membrane model for the determination of anti-angiogenic effects of imatinib. *Eur J Pharm Biopharm* 85, 711-715. doi:10.1016/j.ejpb.2013.07.010
- Pan, Y., Chen, J., Yu, Y. et al. (2018). Enhancement of BMP-2-mediated angiogenesis and osteogenesis by 2-N,6-O-sulfated chitosan in bone regeneration. *Biomater Sci* 6, 431-439. doi:10.1039/C7BM01006K
- Pandit, J., Sultana, Y. and Aqil, M. (2017). Chitosan-coated PLGA nanoparticles of bevacizumab as novel drug delivery to target retina: Optimization, characterization, and in vitro toxicity evaluation. *Artif Cells Nanomed Biotechnol* 45, 1397-1407. doi:10.1080/21691401.2016.1243545
- Pardanaud, L., Altmann, C., Kitos, P. et al. (1987). Vasculogenesis in the early quail blastodisc as studied with a monoclonal antibody recognizing endothelial cells. *Development* 100, 339-349. <http://dev.biologists.org/content/develop/100/2/339.full.pdf>
- Poonguzhali, R., Khaleel Basha, S. and Sugantha Kumari, V. (2018). Novel asymmetric chitosan/PVP/nanocellulose wound dressing: In vitro and in vivo evaluation. *Int J Biol Macromol* 112, 1300-1309. doi:10.1016/j.ijbiomac.2018.02.073
- Rashidi, H. and Sottile, V. (2009). The chick embryo: Hatching a model for contemporary biomedical research. *Bioessays* 31, 459-465. doi:10.1002/bies.200800168
- Ribatti, D., Vacca, A., Roncali, L. and Dommacco, F. (1996). The chick chorioallantoic membrane as a model for in vivo research on angiogenesis. *Int J Dev Biol* 40, 1189-1197. <http://www.ijdb.ehu.es/web/paper.php?doi=9032025>
- Ribatti, D., Nico, B., Vacca, A. and Presta, M. (2006). The gelatin sponge – Chorioallantoic membrane assay. *Nat Protoc* 1, 85-91. doi:10.1038/nprot.2006.13
- Ribatti, D. (2016). The chick embryo chorioallantoic membrane (CAM). A multifaceted experimental model. *Mech Dev* 141, 70-77. doi:10.1016/j.mod.2016.05.003



- Sedmera, D. and McQuinn, T. (2008). Embryogenesis of the heart muscle. *Heart Fail Clin* 4, 235-245. doi:10.1016/j.hfc.2008.02.007
- Shah, U. H., Gonjari, G. R. and Patil, A. E. (2014). Angiostatic property of chitosan acetate in the chick chorioallantoic membrane (CAM), in ovo. *Bioscan* 9, 1505-1508. http://www.thebioscan.in/Journals_PDF/9426%20U%20H%20SAHA_3186.pdf
- Shahzadi, L., Yar, M., Jamal, A. et al. (2016). Triethyl orthoformate covalently cross-linked chitosan-(poly vinyl) alcohol based biodegradable scaffolds with heparin-binding ability for promoting neovascularization. *J Biomater Appl* 31, 582-593. doi:10.1177/0885328216650125
- Singh, S., Wu, B. M. and Dunn, J. C. (2012). Delivery of VEGF using collagen-coated polycaprolactone scaffolds stimulates angiogenesis. *J Biomed Mater Res A* 100, 720-727. doi:10.1002/jbm.a.34010
- Steffens, L., Wenger, A., Stark, G. B. and Finkenzeller, G. (2009). In vivo engineering of a human vasculature for bone tissue engineering applications. *J Cell Mol Med* 13, 3380-3386. doi:10.1111/j.1582-4934.2008.00418.x
- Stegen, S., van Gestel, N. and Carmeliet, G. (2015). Bringing new life to damaged bone: The importance of angiogenesis in bone repair and regeneration. *Bone* 70, 19-27. doi:10.1016/j.bone.2014.09.017
- Stocum, D. L. (2002). Regenerative biology and medicine. *J Musculoskelet Neuronal Interact* 2, 270-273. <http://www.ismni.org/jmni/pdf/7/Stocum.pdf>
- Strick, D. M., Waycaster, R. L., Montani, J. P. et al. (1991). Morphometric measurements of chorioallantoic membrane vascularity: Effects of hypoxia and hyperoxia. *Am J Physiol* 260, H1385-1389. doi:10.1152/ajpheart.1991.260.4.H1385
- Tai, H. Y., Fu, E., Cheng, L. P. and Don, T. M. (2014). Fabrication of asymmetric membranes from polyhydroxybutyrate and biphasic calcium phosphate/chitosan for guided bone regeneration. *J Polym Res* 21, 421. doi:10.1007/s10965-014-0421-8
- Tan, M. L., Shao, P., Friedhuber, A. M. et al. (2014). The potential role of free chitosan in bone trauma and bone cancer management. *Biomaterials* 35, 7828-7838. doi:10.1016/j.biomaterials.2014.05.087
- Tay, S. M., Heng, P. S. and Chan, L. W. (2012). The chick chorioallantoic membrane imaging method as a platform to evaluate vasoactivity and assess irritancy of compounds. *J Pharm Pharmacol* 64, 1128-1137. doi:10.1111/j.2042-7158.2012.01506.x
- Tomco, M., Petrovova, E., Giretova, M. et al. (2017). In vitro and in vivo study of microporous ceramics using MC3T3 cells, CAM assay and a pig animal model. *Anat Sci Int* 92, 569-580. doi:10.1007/s12565-016-0362-x
- Valdes, T. I., Kreutzer, D. and Moussy, F. (2002). The chick chorioallantoic membrane as a novel in vivo model for the testing of biomaterials. *J Biomed Mater Res* 62, 273-282. doi:10.1002/jbm.10152
- Vargas, G. E., Durand, L. A., Cadena, V. et al. (2013). Effect of nano-sized bioactive glass particles on the angiogenic properties of collagen based composites. *J Mater Sci Mater Med* 24, 1261-1269. doi:10.1007/s10856-013-4892-7
- Veleirinho, B., Coelho, D. S., Dias, P. F. et al. (2012). Nanofibrous poly(3-hydroxybutyrate-co-3-hydroxyvalerate)/chitosan scaffolds for skin regeneration. *Int J Biol Macromol* 51, 343-350. doi:10.1016/j.ijbiomac.2012.05.023
- Wang, X., Li, Q., Hu, X. et al. (2012). Fabrication and characterization of poly(L-lactide-co-glycolide) knitted mesh-reinforced collagen-chitosan hybrid scaffolds for dermal tissue engineering. *J Mech Behav Biomed Mater* 8, 204-215. doi:10.1016/j.jmbbm.2012.01.001
- Wang, Y. W., Yang, F., Wu, Q. et al. (2005). Effect of composition of poly(3-hydroxybutyrate-co-3-hydroxyhexanoate) on growth of fibroblast and osteoblast. *Biomaterials* 26, 755-761. doi:10.1016/j.biomaterials.2004.03.023
- Yu, W. L., Sun, T. W., Qi, C. et al. (2017). Enhanced osteogenesis and angiogenesis by mesoporous hydroxyapatite microspheres-derived simvastatin sustained release system for superior bone regeneration. *Sci Rep* 7, 44129. doi:10.1038/srep44129
- Zhang, J., Deng, A., Yang, Y. et al. (2015). HPLC detection of loss rate and cell migration of HUVECs in a proanthocyanidin cross-linked recombinant human collagen-peptide (RHC)-chitosan scaffold. *Mater Sci Eng C Mater Biol Appl* 56, 555-563. doi:10.1016/j.msec.2015.07.019

Conflict of interest

There is no conflict of interest.

Acknowledgements

The present study was supported in part by the Grant Agency of Ministry of the Education, Science, Research and Sport of the Slovak Republic no. VEGA-1/0046/16; Slovak Research and Development Agency under the contract no. APVV-17-0110; Ministry of Education, Youth and Sports of the Czech Republic PROGRESS-Q38, Charles University SVV Graduate Student Training Program; Ministry of Health AZV CR, 15-32497A, 17-28265A; Czech Academy of Sciences RVO: 67985823, INTER-COST LTC17023, and LM2015062 Czech-BioImaging CZ.02.1.01/0.0/0.0/16_013/0001775 Modernization and support of research activities of the national infrastructure for biological and medical imaging Czech-BioImaging funded by OP RDE.

The authors would like to thank Blanka Topinková and Mariana Saulicova from the Institute of Anatomy, Charles University in Prague, Czech Republic and the Institute of Anatomy, University of Veterinary Medicine and Pharmacy in Kosice, Slovak Republic, for their laboratory facilities.